Malaysian Journal of Mathematical Sciences 19(1): 177–205 (2025)
https://doi.org/10.47836/mjms.19.1.10

Malaysian Journal of Mathematical Sciences

Journal homepage: https://mjms.upm.edu.my

Stability and Control of a Vector-Host Disease Model with Time Delay and Saturated Treatment

Jothika, S.[1] and Radhakrishnan, M.*[1,2]

[1]*Department of Mathematics, College of Engineering and Technology, SRM Institute of Science and Technology, Kattankulathur - 603203, India*
[2]*Directorate of Learning and Development, SRM Institute of Science and Technology, Kattankulathur - 603203, India*

E-mail: rakrims@gmail.com
**Corresponding author*

Received: 17 July 2024
Accepted: 18 November 2024

Abstract

This paper studies the dynamics of a vector-host illness model with a time-based delay and a saturated treatment function. The human population is divided into three compartments, while the vector population is categorized into two groups. A treatment function is introduced to account for the limited capacity of the healthcare system. Four control strategies are identified to reduce the infected population and increase the number of susceptible and recovered individuals. The analysis demonstrates endemic and disease-free equilibria exhibit stability depending on the basic reproduction number. Additionally, the study addresses optimal control with time delays, revealing the impact of delayed therapies on disease dynamics and control strategies. Numerical simulations are used to support and complement the theoretical conclusions.

Keywords: vector-host disease model; saturated treatment function; disease-free equilibrium; global stability, basic reproduction number.

1 Introduction

Mathematical modeling is an essential tool for understanding the dynamics of infectious diseases, particularly vector-borne diseases, which pose a significant global health threat. Diseases such as Malaria, dengue, Zika, and chikungunya account for millions of infections and deaths annually. Vectors, including mosquitoes, ticks, and flies, serve as critical biological agents that transmit infectious pathogens between humans or from animals to humans. The value of mathematical models lies in their ability to simulate these transmission processes, offering insights into the interactions between vectors and host populations. Such models are crucial for formulating and assessing control strategies aimed at reducing the spread of infections. Specifically, models that incorporate saturated treatment functions provide a more realistic representation of healthcare systems, which often face limitations in treatment capacities. By accounting for these constraints, the models allow for more accurate predictions and evaluations of control measures [19].

Vector-borne diseases disproportionately affect vulnerable populations, particularly children in developing nations, emphasizing the urgent need for a comprehensive understanding of vector-host dynamics and the development of effective intervention strategies. Recent studies have demonstrated the practical value of mathematical models in addressing real-world infectious disease challenges. These models extend to the analysis of complex diseases under varying conditions, offering valuable theoretical and empirical insights for public health authorities. For example, a stochastic HTLV-I infection model highlighted the role of environmental noise in determining disease extinction or persistence through the stochastic reproduction number, emphasizing the importance of stochasticity in infection dynamics [6]. Similarly, a fractional-order two-patch tuberculosis model showed that population movement and backward bifurcation affect disease progression, with the disease-free equilibrium being globally stable when $R_0 \leq 1$, and the fractional order α reflecting disease awareness [15]. Additionally, a nonlinear model combining vaccination and media awareness as controls demonstrated, through optimal control theory, that hyperbolic impact functions effectively mitigate infections and reduce epidemic costs [23].

Optimal control theory has emerged as a powerful mathematical framework in disease modeling, playing a significant role in informing public health decisions. By applying mathematical optimization techniques, researchers can identify the most effective intervention methods-such as vaccination, treatment, and quarantine while accounting for resource limitations. Optimal control techniques have been used to guide immunization programs by determining the best timing and distribution of vaccines to efficiently reduce the spread of infections [24]. These methods are particularly useful in regions with limited healthcare resources, where efficient allocation is essential for achieving the greatest impact. Studies have shown that optimal control approaches can significantly improve intervention effectiveness in various vector-borne diseases, including Zika and dengue, where temporal dynamics and spatial factors play critical roles in disease transmission [21]. Understanding these temporal dynamics, how the number of cases changes over time and how interventions can alter these trends is crucial for designing effective outbreak prevention strategies.

The global burden of vector-borne diseases has increased considerably over the past few decades. Dengue, in particular, has become one of the fastest-spreading mosquito-borne viral diseases globally. Before 1970, dengue outbreaks were reported in only nine countries; by 1995, that number had more than doubled, and the disease continues to spread into new regions. According to the World Health Organization (WHO), there are 50 to 100 million cases of dengue fever annually, with around $10,000$ children dying each year from dengue-related hemorrhaging. The severity of dengue outbreaks highlights the need for effective mathematical models to better understand

transmission dynamics and develop control strategies. Models incorporating time delays have been particularly useful in this context, as they account for biological and logistical delays in the disease transmission process such as the incubation period of the virus within mosquitoes and humans or the time required for interventions to take effect [28].

In addition to time delays, demographic structures must also be considered in disease modeling to capture the complexity of real-world transmission dynamics. Factors such as population density, age distribution, and movement patterns significantly influence the spread of vector-borne diseases. For example, models that incorporate demographic structures provide more accurate predictions of disease spread in urban and rural settings, where population dynamics and human-vector interaction rates vary significantly [14]. Recent studies in disease modeling have integrated nonlinear dynamics, backward bifurcation, and optimal control measures, providing deeper insights into vector-host interactions and effective intervention strategies. A deterministic dengue model, calibrated with data from the 2017 Peshawar outbreak, estimated the basic reproduction number and optimized insecticide and vaccination strategies, revealing their cost-based trade-offs in infection control [3].

For COVID-19, a model incorporating environmental contamination and vaccination demonstrated that increased vaccination and reduced contamination significantly lower the reproduction number, while seasonal effects prolong persistence [20]. A nine-stage COVID-19 model for India highlighted the importance of early pharmaceutical and non-pharmaceutical interventions in flattening peaks and minimizing control costs [18]. Similarly, a nonlinear model showed that environmental contamination amplifies infections, while effective sanitization ensures stability if the reproduction number falls below one [27]. A compartmental SAIQJR model underscored that combining pharmaceutical and non-pharmaceutical controls achieves better epidemic mitigation compared to isolated strategies [22]. Lastly, a novel numerical method combining spectral collocation and parametric iteration accurately solves nonlinear optimal control problems, demonstrating effectiveness across various applications [4].

Biswas et al. [9] analyzed SEIR models with vaccination constraints, showing the impact of limited vaccine availability on disease control. Aldila et al. [5] demonstrated the effectiveness of mosquito repellent treatments in controlling Dengue outbreaks through optimal control strategies. Dwivedi et al. [12] calibrated a nonlinear vector-host model for dengue, highlighting vaccination and treatment role in reducing infections and hospitalizations. Ratti and Kalra [25] modeled Malaria and Rotavirus co-infection dynamics, showing global stability at the disease-free equilibrium and the benefits of combined control measures. Bera et al. [7] studied an HTLV-I model, identifying stability conditions and Hopf bifurcation dynamics, with sensitivity analysis emphasizing key transmission parameters.

Understanding vector-host dynamics is crucial for controlling vector-borne diseases. The concept of backward bifurcation, for example, illustrates how complex interactions between disease transmission and treatment efforts can lead to multiple equilibrium points, complicating control efforts. Additionally, models that incorporate saturated treatment functions, which account for the limited capacity of healthcare systems provide a more realistic representation of control efforts in practice [26]. Such models highlight the need for timely and effective interventions, as delays or insufficient responses can result in severe outbreaks.

Human-vector interactions, particularly mosquito bites, are pivotal in the transmission of vector-borne diseases such as Malaria and dengue. Wang et al. [31] analyzed a model with age-stratified host and vector populations, identifying stability conditions for infection-free and endemic equilibria based on the basic reproduction number. Thongsripong et al. [29] emphasized the variability in mosquito biting rates, challenging traditional assumptions and highlighting the need for

empirical data to refine models of vector-borne disease transmission. Bera et al. [8] introduced a fuzzy mathematical model for HTLV-I infection, exploring stability and persistence under imprecise biological parameters, with numerical simulations validating the theoretical results. Mondal and Khajanchi [22] underscored the significance of incorporating ecological, social, and spatial heterogeneity into mosquito-borne disease models to enhance intervention strategies. Khajanchi et al. [17] developed a COVID-19 model integrating pharmaceutical and non-pharmaceutical interventions, demonstrating their combined effectiveness in reducing transmission and flattening epidemic peaks through optimal control methods.

Human mobility significantly influences the spatial and temporal dynamics of vector-borne disease outbreaks. Acevedo et al. [1] demonstrated that while human movement reduces the basic reproduction number R_0 in spatially heterogeneous settings, it can initially increase infection prevalence by reducing exposure heterogeneity before ultimately lowering prevalence at high mobility rates. Eder et al. [13] identified critical gaps in understanding urban vector-borne disease (VBD) transmission, such as the roles of asymptomatic carriers, co-infections, and socioeconomic factors, emphasizing the need for more comprehensive models. Das et al. [11] explored TB transmission with re-infections, showing that backward bifurcation occurs when $R_0 < 1$, making eradication contingent on reducing R_0 below a critical threshold. Adams and Kapan [2] analyzed the effects of structured human movement on dengue transmission using a metapopulation model, highlighting the emergence of infection hubs due to frequent short human visits and advocating for integrated public health strategies. Khajanchi et al. [16] investigated CD8+ T-cell responses to HTLV-I infection, identifying three steady states governed by reproduction numbers R_0 and R_1, with implications for HTLV-I pathogenesis and HAM/TSP progression.

In Section 2, we examine a mathematical model that captures the interactions between vectors and hosts, incorporating time delays to account for biological lags in disease transmission and intervention effects. In Section 3, stability analysis is performed to determine equilibrium points, while optimal control techniques are applied to design intervention strategies that minimize disease spread. The novelty of this approach lies in incorporating time delay and a saturated treatment function, which provides a more realistic representation of healthcare system capacity limitations. This framework enhances our understanding of how delayed responses and treatment constraints impact the overall dynamics of vector-borne diseases, offering new insights into effective disease control strategies.

2 Model Construction

Time delay is incorporated into the dynamics of the vector-host illness, and indicate the whole population of humans by $N_H(t)$, which can be further subdivided into three distinct classes: susceptible humans $S_H(t)$, infected humans $I_H(t)$, and recovered humans $R_H(t)$ at any given time t. Therefore, $N_H(t) = S_H(t) + I_H(t) + R_H(t)$. A delay parameter τ is incorporated into the differential equation governing the dynamics of sensitive individuals to account for the time delay effect (S_H),

$$\frac{dS_H}{dt}(t) = \Lambda_H - \frac{\beta_1 S_H(t-\tau) I_V(t-\tau)}{1+\alpha_1 I_V(t-\tau)} - \mu_H S_H(t), \tag{1}$$

where τ represents the time-based delay, capturing the lag in the response of susceptible humans to changes in the infection dynamics caused by infected vectors (I_V). This delay reflects the time it takes for individuals to become infected after contact with infected vectors and subsequently contribute to the pool of infected humans. Incorporating time delay into mathematical models

of vector-host diseases is crucial for accurately representing the temporal dynamics of disease transmission and better analyzing how control strategies affect the management and spread of illness. The dynamics of infected humans (I_H), while accounting for the treatment function, are modeled with the addition of a delay parameter τ to the differential equation,

$$\frac{dI_H}{dt}(t) = \frac{\beta_1 S_H(t-\tau) I_V(t-\tau)}{1+\alpha_1 I_V(t-\tau)} - (\mu_H + \delta_H) I_H(t) - \frac{\gamma u I_H(t)}{1+buI_H(t)}. \tag{2}$$

The delay in the response of infected humans to changes in the infection dynamics due to infected vectors (I_V) and the treatment function. The treatment function, described by the term $\frac{\gamma}{1+buI_H}$, is essential for predicting the dynamics of illness. It reflects the capacity of the healthcare system to provide treatment, where $\frac{\gamma}{b}$ is the maximum amount of medical resources available in a given amount of time, and $\frac{1}{1+buI_H}$ explains the impact of afflicted people delaying getting treatment. The effectiveness of control methods and the disease spread in a real-world setting require a more accurate portrayal of the temporal dynamics of disease transmission and treatment, which is made possible by the inclusion of time delay along with the treatment function. Based on the treatment function and natural death, the differential equation can be modified to represent the dynamics of the recovered human population (RH),

$$\frac{dR_H}{dt}(t) = \frac{\gamma u I_H(t-\tau)}{1+buI_H(t-\tau)} - \mu_H R_H(t). \tag{3}$$

The temporal aspect of how the recovery process responds to changes in the prevalence of infected humans (I_H). This time delay can be crucial in simulating the dynamics of vector-host illnesses and comprehending the effects of time delays on disease control and management, since it represents the lag in the effect of therapy on the recovery of infected persons. Considering the contact rates with infected humans, the differential equation for the susceptible vector population (S_V) can be revised as follows,

$$\frac{dS_V}{dt}(t) = \Lambda_V - \frac{\beta_2 S_V(t-\tau) I_H(t-\tau)}{1+\alpha_2 I_H(t-\tau)} - \mu_V S_V(t), \tag{4}$$

where τ represents the time-based delay, signifying the lag in the response of susceptible vectors to changes in infection dynamics caused by infected humans. The term $\frac{\beta_2 S_V(t-\tau) I_H(t-\tau)}{1+\alpha_2 I_H(t-\tau)}$ accounts for the delayed effect of contact between susceptible vectors and infected humans, with α_2 being the saturation constant. A more realistic depiction of the temporal dynamics in the interaction between susceptible vectors and infected people is possible by include time delay in the susceptible vector population equation. To offer a more precise model for the spread of illnesses including vectors and hosts, it is imperative to comprehend how temporal delays affect the response of susceptible vectors to infection dynamics. The dynamics of the infected vector population (I_V), taking into account the frequency of interaction with infected humans (I_H), can be modified in the differential equation as follows,

$$\frac{dI_V}{dt}(t) = \frac{\beta_2 S_V(t-\tau) I_H(t-\tau)}{1+\alpha_2 I_H(t-\tau)} - \mu_V I_V(t). \tag{5}$$

Signifying time lag into the response of infected vectors to changes in infection dynamics caused by infected humans. The temporal dynamics in the interaction between infected vectors and infected people can be more accurately represented by adding time delay to the infected vector population equation. Introducing time delay into the system of (1)−(5) account for the temporal aspects of

disease transmission. For each compartment, a time delay parameter τ is included to represent the lag in the response of each population to changes in infection dynamics,

$$\begin{aligned}
\frac{dS_H}{dt}(t) &= \Lambda_H - \frac{\beta_1 S_H(t-\tau) I_V(t-\tau)}{1+\alpha_1 I_V(t-\tau)} - \mu_H S_H(t),\\
\frac{dI_H}{dt}(t) &= \frac{\beta_1 S_H(t-\tau) I_V(t-\tau)}{1+\alpha_1 I_V(t-\tau)} - (\mu_H+\delta_H) I_H(t) - \frac{\gamma u I_H(t)}{1+buI_H(t)},\\
\frac{dR_H}{dt}(t) &= \frac{\gamma u I_H(t-\tau)}{1+buI_H(t-\tau)} - \mu_H R_H(t),\\
\frac{dS_V}{dt}(t) &= \Lambda_V - \frac{\beta_2 S_V(t-\tau) I_H(t-\tau)}{1+\alpha_2 I_H(t-\tau)} - \mu_V S_V(t),\\
\frac{dI_V}{dt}(t) &= \frac{\beta_2 S_V(t-\tau) I_H(t-\tau)}{1+\alpha_2 I_H(t-\tau)} - \mu_V I_V(t),
\end{aligned} \tag{6}$$

where the description of parameters can be refer to Table 1. A more accurate depiction of the dynamics is possible by include time delays in each equation, which take into consideration how long it takes for each population to react to variations in the dynamics of the infection. This modification is required to provide a more realistic model for studying the spread of disease and its treatment, as well as to correctly depict the temporal characteristics of disease transmission from vectors to hosts.

Table 1: Description of parameters.

Parameter	Description
Λ_H	Birth rate of susceptible humans
β_1	Rate of transmission of the infection from vulnerable individuals to infected vectors
α_1	Saturated factor for the interaction between infected vectors and susceptible humans
μ_H	The natural death rate among people
δ_H	Human mortality rate from disease
γ	Recovery rate of humans
u	Control parameter influencing the spread of the infection from susceptible to infected persons
b	Rate of infection transmission from susceptible to infected persons
Λ_V	Suppression rate of vulnerable vectors
β_2	Transmission rate from infected humans to susceptible vectors
α_2	Saturation factor for the relationship between susceptible vectors and sick people
μ_V	Natural mortality rate of vectors

The initial conditions are as follows when adding time delay to the set of equations:

$$S_H(0) \geq 0, \quad I_H(0) \geq 0, \quad R_H(0) \geq 0, \quad S_V(0) \geq 0, \quad I_H(0) \geq 0. \tag{7}$$

These prerequisites guarantee that at the beginning time point, the values of all population are non-negative. Each population react to variations in the dynamics of infection is behind due to the temporal delay. Nevertheless, the insertion of time delay has no effect on the starting conditions themselves. The physical model interpretation is ensured by the non-negativity requirements, and they reflect the initial values of each population at time $t = 0$. As a result, the beginning circumstances with time delay are the same as previously mentioned, and they are very important in

deciding how the system behaves as it changes over time. Introducing time delay into the equation describing the dynamics of the human population by considering a time delay parameter τ,

$$\frac{dN_H}{dt}(t) = \Lambda_H - \mu_H N_H(t) - \delta_H I_H(t-\tau). \tag{8}$$

The evolution of the human population over time is represented by this equation, accounting for the birth rate (Λ_H), natural death rate (μ_H), and disease-induced death rate (δ_H), with a time delay for the population of diseased humans (I_H). The inequality $\frac{dN_H}{dt}(t) + \mu_H N_H(t) \leq \Lambda_H$ holds, making sure that the rate of increase in the human population (births minus deaths) is bounded by the birth rate Λ_H. This disparity accounts for the effects on total population dynamics of both disease-induced and natural mortality. Introducing time delay into the inequalities with a parameter τ as,

$$\begin{cases} 0 \leq S_H(t), \\ I_H(t), \\ R_H(t) \leq \dfrac{\Lambda_H}{\mu_H}(1 - e^{-\mu_H(t-\tau)}) + \dfrac{N_H}{S_H(0) + I_H(0) + R_H(0)} e^{-\mu_H(t-\tau)}. \end{cases} \tag{9}$$

The term $\frac{\Lambda_H}{\mu_H}(1-e^{-\mu_H(t-\tau)})$ represents the contribution from births and natural deaths up to time $t-\tau$, and the term $\frac{N_H}{S_H(0)+I_H(0)+R_H(0)} e^{-\mu_H(t-\tau)}$ represents the contribution from the initial conditions. By accounting for the delayed impacts of births, deaths, and beginning circumstances on the susceptible, infected, and recovered populations over time, time delay may be incorporated into these inequalities to provide a more thorough understanding of the limitations on the population dynamics. The dynamics of the total vector population $(N_V = S_V + I_V)$ with time delay parameter τ can be modified as,

$$\frac{dN_V}{dt}(t) = \Lambda_V - N_H(t-\tau). \tag{10}$$

The exact solution for this differential equation is,

$$N_V(t) = \frac{\Lambda_V}{\mu_V} + ce^{-\mu_V(t-\tau)}, \tag{11}$$

where c is integration constant. Now, considering the limit as $\tau \to \infty$, the term $e^{-\mu_V(t-\tau)}$ approaches zero, and we obtain,

$$\lim_{t\to 0} N_V(t) = \frac{\Lambda_V}{\mu_V}. \tag{12}$$

Thus, as t approaches infinity, we have $0 \leq N_V \leq \frac{\Lambda_V}{\mu_V}$. The viable area for the suggested model ϕ, considering time delay is

$$\phi = \left\{ (S_H, I_H, R_H, S_V, I_V) \in \mathbb{R}^5 | N_H \leq \frac{\Lambda_H}{\mu_H}, \quad N_V \leq \frac{\Lambda_V}{\mu_V} \right\}. \tag{13}$$

Taking into consideration the birth, death, and time-delayed dynamics, this area establishes the permissible values for the compartments (susceptible, infected, recovered, susceptible vector, and infected vector) in the model.

Lemma 2.1. *The set* $\phi = \left\{ (S_H, I_H, R_H, S_V, I_V) \in \mathbb{R}^5 | N_H \leq \frac{\Lambda_H}{\mu_H}, \quad N_V \leq \frac{\Lambda_V}{\mu_V} \right\}$ *is positively invariant with time delay.*

Proof. The standard comparison theorem can be applied to demonstrate that the set ϕ is said to be positively invariant. Let's consider the following comparison functions,

$$0 \leq N_H(t) \leq N_H(0)e^{-\mu_H t} + \frac{\Lambda_H}{\mu_H}\left(1 - e^{-\mu_H t}\right), \tag{14}$$

$$0 \leq N_V(t) \leq N_V(0)e^{-\mu_V t} + \frac{\Lambda_V}{\mu_V}\left(1 - e^{-\mu_V t}\right). \tag{15}$$

As $t \to \infty$,

$$0 \leq N_H \leq \frac{\Lambda_H}{\mu_H}, \qquad 0 \leq N_V \leq \frac{\Lambda_V}{\mu_V}. \tag{16}$$

$\therefore \phi$ is positively invariant. □

3 The State of Equilibrium and Local Stability

This section analyzes the local stability of the endemic and disease-free equilibria of system (6), incorporating time delays to account for delays in transmission and recovery processes. Time delays are introduced to model the period between exposure and the onset of infectiousness in the human and vector populations, which has significant implications for disease dynamics.

3.1 Disease-free equilibrium

The disease-free equilibrium without time delay is expressed as,

$$P_0 = (S_{0_H}, 0, 0, S_{0_V}, 0) = \left(\frac{\Lambda_H}{\mu_H}, 0, 0, \frac{\Lambda_V}{\mu_V}, 0\right). \tag{17}$$

The incubation period or the delay between exposure and infectiousness in both human and vector populations, modifies the disease-free equilibrium while delay introduced. The modified disease-free equilibrium is,

$$P_0(\tau) = (S_{0_H}(\tau), 0, 0, S_{0_V}(\tau), 0), \tag{18}$$

where $S_{0_H}(\tau)$ and $S_{0_V}(\tau)$ are solutions to the following delay differential equations,

$$S_{0_H}(\tau) = \frac{\Lambda_H}{\mu_H}e^{\mu_H \tau}, \tag{19}$$

$$S_{0_V}(\tau) = \frac{\Lambda_V}{\mu_V}e^{\mu_V \tau}. \tag{20}$$

Thus, the disease-free equilibrium with time delay becomes,

$$P_0(\tau) = \left(\frac{\Lambda_H}{\mu_H}e^{\mu_H \tau}, 0, 0, \frac{\Lambda_V}{\mu_V}e^{\mu_V \tau}, 0\right). \tag{21}$$

The fact that transmission does not occur immediately after exposure, modeling the delayed progression to an infectious state in both human and vector populations when time delay reflects.

3.2 Basic reproduction number R_0

To understand the effect of the time delay on disease transmission, the basic reproduction number R_0 is calculated. Time delays are incorporated into the transmission terms, using the next-generation matrix [19, 27] approach. The transmission matrix becomes,

$$F = \begin{bmatrix} 0 & \beta_1 e^{-\alpha_1 \tau} \\ \dfrac{\Lambda_H}{\mu_H} \beta_2 e^{-\alpha_2 \tau} & 0 \end{bmatrix}, \tag{22}$$

and the transition matrix is given by,

$$V = \begin{bmatrix} \mu_H + \delta_H + \gamma u & 0 \\ 0 & \mu_V \end{bmatrix}. \tag{23}$$

The basic reproduction number R_0, which governs the stability of the disease-free equilibrium is given by,

$$R_0 = \sqrt{\frac{\beta_1 \beta_2 \Lambda_H \Lambda_V}{\mu_H^2 \mu_V (\mu_H + \delta_H + \gamma u)} e^{-(\alpha_1 \tau + \alpha_2 \tau)}}, \tag{24}$$

where the exponential terms $e^{-\alpha_1 \tau}$ and $e^{-\alpha_2 \tau}$ represent the effect of time delays in human-to-vector and vector-to-human transmission. These delays reduce the effective transmission rate, as the period between exposure and becoming infectious is prolonged. This directly impacts the basic reproduction number, making it smaller as the delay increases.

3.3 Local stability of disease-free equilibrium

Theorem 3.1. *The disease-free equilibrium P_0 of the time-delayed system (6) is locally asymptotically stable if $R_0 < 1$.*

Proof. The stability of the disease-free equilibrium depends on the basic reproduction number R_0 [27]. When $R_0 < 1$, the infection cannot sustain itself within the population, meaning each infected individual produces, on average, fewer than one new infection. Despite the time delay in transmission, the system will return to the disease-free equilibrium. As long as $R_0 < 1$, the population remains disease-free in the long run, and the infection dies out. □

3.4 Endemic equilibrium

For $R_0 > 1$, the system admits an endemic equilibrium P_1^*, where the disease persists within the population. The endemic equilibrium is defined by the following set of equations,

$$P_1^* = (S_H^*, I_H^*, R_H^*, S_V^*, I_V^*), \tag{25}$$

with the components of the endemic equilibrium given by,

$$S_H^* = \frac{\delta_H}{buI_H^*+1}\frac{\mu_H}{buI_H^*+1+\gamma u}\frac{I_H^*}{\alpha_1\beta_2\Lambda_V(\beta_2+\alpha_2\mu_V)+\mu_V^2\beta_1\beta_2\Lambda_V(buI_H^*+1)},$$
$$R_H^* = \frac{\gamma u I_H^*}{\mu_H(buI_H^*+1)},$$
$$S_V^* = \frac{\Lambda_V}{\alpha_2 I_H^*+1}\frac{\beta_2 I_H^*+\alpha_2 I_H^*\mu_V}{\beta_2 I_H^*+\alpha_2 I_H^*\mu_V+\mu_V},$$
$$I_V^* = \frac{\beta_2 I_H^*+\alpha_2 I_H^*\mu_V}{\beta_2 I_H^*+\alpha_2 I_H^*\mu_V+\mu_V}.$$

The delayed transmission process impacts the endemic equilibrium, as the time-delay infected both human and vector populations is factored into the system. This means that longer delays lead to a slower rise to endemic levels.

3.5 Stability of the endemic equilibrium

Theorem 3.2. *If $R_0 > 1$, the endemic equilibrium P_1^* of the time-delayed system (6) is locally asymptotically stable.*

Proof. The stability of the endemic equilibrium is determined by examining the Jacobian matrix J^* at P_1^*, incorporating the time delay into the transmission terms. The Jacobian matrix is,

$$J = \begin{bmatrix} J_{11} & 0 & 0 & -\frac{\beta_1 S_H^*(1+\alpha_1 I_V^*)^2}{(1+\alpha_1 I_V^*)^2} & \frac{\beta_1 I_V^*}{1+\alpha_1 I_V^*} \\ 0 & J_{22} & 0 & \frac{\beta_1 S_H^*(1+\alpha_1 I_V^*)^2}{(1+\alpha_1 I_V^*)^2} & 0 \\ 0 & 0 & J_{33} & 0 & 0 \\ 0 & 0 & -\beta_2 S_V^*(1+\alpha_2 I_H^*)^2 & 0 & \frac{-\beta_2 I_H^*}{1+\alpha_2 I_H^*} \\ 0 & 0 & \frac{\beta_1 S_V^*(1+\alpha_1 I_H^*)^2}{(1+\alpha_1 I_H^*)^2} & \frac{\beta_2 I_H^*}{1+\alpha_2 I_H^*} & -\mu_V \end{bmatrix}, \tag{26}$$

where

$$J_{11} = -\mu_H - \frac{\beta_1 I_V^* e^{-\alpha_1\tau}}{1+\alpha_1 I_V^*},$$
$$J_{22} = -\mu_H - \delta_H - \frac{\gamma u(1+buI_H^*)^2}{(1+buI_H^*)^2},$$
$$J_{33} = -\frac{\beta_1 S_H^*(1+\alpha_1 I_V^*)^2}{(1+\alpha_1 I_V^*)^2}.$$

The characteristic equation becomes,

$$\lambda^4 + K_1 e^{-\alpha_1\tau}\lambda^3 + K_2 e^{-\alpha_2\tau}\lambda^2 + K_3 e^{-\alpha_1\tau}\lambda + K_4 e^{-b\tau} = 0, \tag{27}$$

where the coefficients K_1, K_2, K_3, K_4 are given by,

$$K_1 = \frac{\mu_H^* + m_1 + m_5}{Q_1 + 2\mu_V} > 0,$$

$$K_2 = \frac{\mu_H^*(m_5 + Q_1) + m_4(\mu_H^* + Q_1 + \mu_V^*)}{2\mu_V(\mu_H^* + m_5 + Q_1)} + \frac{m_1(m_4 + m_5 + Q_1 + 2\mu_V)}{\mu_V^2 + (m_4 m_5 - m_2 m_3)e^{-\alpha_1 \tau}},$$

$$K_3 = \frac{m_4 e^{-\alpha_1 \tau}}{Q_1 \mu_H + \mu_V(\mu_H + Q_1)} + \frac{\mu_V^2 e^{-\alpha_1 \tau}}{2\mu_H(m_5 + Q_1 + \mu_V) + \mu_V(2(m_5 + Q_1) + \mu_V) + (m_4 m_5 - m_2 m_3)}(\mu_H + \mu_V),$$

$$K_4 = \frac{\mu_V e^{-\alpha_1 \tau}}{\mu_H((m_5 + Q_1)\mu_V + m_4 Q_1) + m_1(m_5 + Q_1)(m_4 + \mu_V) + (m_4 m_5 - m_2 m_3)e^{-\alpha_1 \tau}} \mu_H \mu_V.$$

Here, the coefficients $m_1, m_2, m_3, m_4, m_5, Q_1$ represent various transmission and recovery rates,

$$m_1 = \beta_1 I_V^* \frac{1}{1 + \alpha_1 I_V^*} e^{-\alpha_1 \tau},$$

$$m_2 = \beta_2 S_V^* \frac{1}{1 + \alpha_2 I_H^*} e^{-\alpha_2 \tau},$$

$$m_3 = \beta_1 S_H^* \frac{1}{1 + \alpha_1 I_V^*} e^{-\alpha_1 \tau} \frac{1}{(1 + \alpha_1 I_V^*)^2} e^{-\alpha_1 \tau},$$

$$m_4 = \beta_2 I_H^* \frac{1}{1 + \alpha_2 I_H^*} e^{-\alpha_2 \tau},$$

$$m_5 = \gamma u \frac{1}{1 + b u I_H^*} e^{-b\tau},$$

$$Q_1 = \delta_H + \mu_H.$$

The condition $(m_4 m_5 - m_2 m_3) > 0$ ensures that all the coefficients K_1, K_2, K_3, K_4 are positive. Satisfying the Routh-Hurwitz criteria guarantees that the endemic equilibrium P_1^* is locally asymptotically stable, even when time delay is incorporated into the transmission dynamics. □

4 Backward Bifurcation's Development

The bifurcation parameter β_1 for the system (6) is examined. At the critical point $R_0 = 1$, the expression for β_1 accounting for time delay becomes,

$$\beta_1 = \frac{\mu_H \mu_V^2 (\delta_H + \mu_H + \gamma u)}{\beta_2 \Lambda_H \Lambda_V e^{-\alpha_1 \tau}}. \tag{28}$$

This modified expression for β_1 reflects the delayed progression to infectiousness in both the human and vector populations. Time delay introduces an exponential factor, which reduces the effective transmission rate and alters the bifurcation behavior by shifting the bifurcation threshold.

To analyze the system dynamics, the variables are transformed into y_1, y_2, y_3, y_4, y_5, and the system

is represented as $\frac{dy}{dt} = f$, where $f = (f_1, f_2, f_3, f_4, f_5)$ is given by,

$$\begin{aligned}
\frac{dy_1}{dt} &= \Lambda_H - \frac{\beta_1 y_1 y_5}{1+\alpha_1 y_5} e^{-\tau\mu_H} - \mu_H y_1, \\
\frac{dy_2}{dt} &= \frac{\beta_1 y_1 y_5}{1+\alpha_1 y_5} e^{-\tau\mu_H} - (\mu_H + \delta_H) y_2 - \frac{\gamma u y_2}{1+buy_2}, \\
\frac{dy_3}{dt} &= \frac{\gamma u y_2}{1+buy_2} e^{-\tau\mu_H} - \mu_H y_3, \\
\frac{dy_4}{dt} &= \Lambda_V - \frac{\beta_2 y_4 y_2}{1+\alpha_2 y_2} e^{-\tau\mu_V} - \mu_V y_4, \\
\frac{dy_5}{dt} &= \frac{\beta_2 y_4 y_2}{1+\alpha_2 y_2} e^{-\tau\mu_V} - \mu_V y_5.
\end{aligned} \tag{29}$$

Time delays τ_{μ_h} and τ_{μ_v} are introduced for μ_H and μ_V, respectively. The Jacobian matrix for the system becomes,

$$J = \begin{bmatrix}
J_{11} & 0 & 0 & 0 & J_{15} \\
J_{21} & -(\mu_H + \delta_H) & 0 & -\dfrac{\gamma u}{(1+buy_2)^2 e^{-\tau_{\mu_h}\mu_H}} & 0 \\
0 & 0 & u\gamma - \mu_H & 0 & 0 \\
0 & 0 & 0 & -\mu_V e^{-\tau_{\mu_v}\mu_V} & 0 \\
0 & 0 & 0 & \dfrac{\beta_2 y_2}{1+\alpha_2 y_2} e^{-\tau_{\mu_v}\mu_V} & -\mu_V e^{-\tau_{\mu_v}\mu_V}
\end{bmatrix}, \tag{30}$$

where

$$\begin{aligned}
J_{11} &= -\mu_H e^{-\tau_{\mu_h}\mu_H}, \\
J_{15} &= -(u\gamma + \delta_H + \mu_H)\mu_V^2 \beta_2 \Lambda_V e^{-\tau_{\mu_v}\mu_V}, \\
J_{21} &= \frac{\beta_1 y_5}{(1+\alpha_1 y_5)^2 e^{-\tau_{\mu_h}\mu_H}}.
\end{aligned}$$

The eigenvectors reflect the influence of time delay on the system dynamics and the modified right eigenvectors are

$$v_1 = 0, \quad v_3 = 0, \quad v_4 = 0, \quad v_5 = \frac{v_2 \mu_V}{\beta_2 \Lambda_V (\delta_H + \gamma_H + \gamma u) e^{-\tau_{\mu_v}\mu_V}}, \quad v_2 = v_2 > 0.$$

The modified left eigenvectors are

$$\begin{aligned}
W_1 &= -W_2 \frac{1}{\delta_H + \mu_H} e^{-\tau_{\mu_h}\mu_H}, \\
W_3 &= \frac{\gamma u}{\mu_H} e^{-\tau_{\mu_h}\mu_H}, \\
W_4 &= -\frac{\beta_2 \Lambda_V}{\mu_V^2} e^{-\tau_{\mu_v}\mu_V}, \\
W_5 &= \frac{\beta_2 \Lambda_V}{\mu_V^2} e^{-\tau_{\mu_v}\mu_V}, \\
W_2 &= W_4 > 0.
\end{aligned}$$

Time delay modifies the expressions for the bifurcation coefficients a_1 and b_1,

$$a_1 = -\frac{2v_2W_2}{\mu_V^2}\left[\frac{\mu_H\mu_V}{\beta_2\Lambda_H\Lambda_V}G_1 + \alpha_1\beta_1\beta_2\frac{\mu_H\mu_V^4}{\mu_V}e^{-\tau_{\mu_h}\mu_H}\right], \tag{31}$$

where

$$G_1 = \mu_H\mu_V e^{-\tau_{\mu_h}\mu_H}\left[\frac{\mu_V}{\alpha_2 Z'} - b\gamma u e^{-\tau_{\mu_v}\mu_V} + \beta_2 Z' e^{-\tau_{\mu_v}\mu_V} + \beta_1\beta_2\Lambda_V Z' e^{-\tau_{\mu_v}\mu_V}\right],$$
$$Z' = \delta_H + \mu_H + \gamma u.$$

The expression for b_1 is

$$b_1 = \frac{\beta_2 v_2 W_2 \Lambda_H \Lambda_V}{\mu_H\mu_V^2}e^{-\tau_{\mu_v}\mu_V}. \tag{32}$$

For backward bifurcation occur, both a_1 and b_1 must be positive. In this case, however, a_1 is negative due to the time delay, preventing backward bifurcation. The negative value of a_1 indicates that the time delay in the transmission process weakens the conditions for multiple stable equilibria to coexist.

5 Lyapunov Approach for Global Stability of Disease-Free Equilibrium

This section examines the global stability of the model (6) by defining a Lyapunov function [27] to assess the stability of the disease-free equilibrium. The analysis incorporates time delays in both the human and vector populations, specifically associated with μ_H and μ_V. The following theorem presents the main result for the global stability of the disease-free equilibrium.

Theorem 5.1. *The disease-free equilibrium of model (6), taking into account the effects of time delays associated with μ_H and μ_V, is globally asymptotically stable if $R_0 < 1$ and unstable otherwise.*

Proof. To prove this result, the following Lyapunov function is defined for the disease-free equilibrium,

$$L(t) = U - S_0^h - S_0^h I_H\frac{S_H}{S_0^h} + \beta_2 S_0^v I_H + Z\left(\frac{S_V - S_0^v}{S_0^v}\right) - S_0^v - S_0^v I_V\frac{S_V}{S_0^v} + ZI_V, \tag{33}$$

where

$$U = \beta_2 S_0^v\left(\frac{S_H - S_0^h}{S_0^h}\right),$$
$$Z = \delta_H + \mu_H + \gamma u.$$

The Lyapunov function $L(t)$ captures the deviation of the state variables from their disease-free equilibrium values. The terms involving S_H, S_V, and I_H represent the delayed effects in the dynamics of the human and vector populations. The function $L(t)$ is structured to ensure that its time derivative is negative for $R_0 < 1$. Taking the time derivative of $L(t)$ using the system (6), the

following expression is obtained,

$$L_0(t) = \beta_2 S_0^v \left(\frac{S_H - S_0^h}{S_0^h}\right) - \frac{S_0^h}{S_H}\Lambda_H - \mu_H S_H - \beta_2 S_0^v \left(\frac{S_H - S_0^h}{S_0^h}\right)\frac{\beta_1 S_H I_V}{1+\alpha_1 I_V} - \beta_2 S_0^v \frac{\beta_1 S_H I_V}{1+\alpha_1 I_V}$$
$$- (\mu_H + \delta_H + \gamma u)\beta_2 S_0^v \frac{\beta_1 S_H I_V}{1+\alpha_1 I_V} + (\mu_H + \delta_H + \gamma u)\beta_2 S_0^v \frac{\beta_2 S_0^v (S_H + I_H + R_H)}{\beta_2 \Lambda_V}$$
$$- \mu_V S_V - (\mu_H + \delta_H + \gamma u)\beta_2 S_0^v \frac{\beta_2 S_0^v (S_H + I_H + R_H)}{\beta_2 \Lambda_V}\frac{\beta_1 S_H I_V}{1+\alpha_1 I_V}. \tag{34}$$

Substituting $S_0^h = \dfrac{\Lambda_H}{\mu_H}$ and $S_0^v = \dfrac{\Lambda_V}{\mu_V}$, and simplifying the terms, the following expression for $L_0(t)$ is obtained,

$$L_0(t) = -\beta_2 \Lambda_V \frac{\mu_H}{\mu_V}\left(\frac{S_H(t-\tau_1) - S_0^h}{S_0^h}\right)^2 S_H(t-\tau_1) - \mu_V Z \left(\frac{S_V(t-\tau_2) - S_0^v}{S_0^v}\right) S_V(t-\tau_2)$$
$$- \beta_2 S_0^v bu(\mu_H + \delta_H)\frac{I_H(t-\tau_1)^2}{1 + buI_H(t-\tau_1)} - Z\mu_V \alpha_1 \frac{I_V(t-\tau_2)^2}{(1+\alpha_1 I_V(t-\tau_2))^2}$$
$$- \frac{I_V(t-\tau_2)(1+\alpha_1 I_V(t-\tau_2))Z\mu_V(1-R_0^2)}{1+\alpha_1 I_V(t-\tau_2)}, \tag{35}$$

where delay is introduced in the Lyapunov function $L_0(t)$, it can be observed that $L_0(t)$ is negative if $R_0 < 1$, and $L_0(t) = 0$ if $S_H = S_0^h$, $S_V = S_0^v$, $I_H = I_V = 0$. Therefore, the largest collection of compact invariants $(S_H, I_H, R_H, S_V, I_V) \in \Phi : L_0(t) = 0$, proving global asymptotic stability of the disease-free equilibrium. □

6 Global Stability and Endemic Equilibrium

The delayed system (6) considering and reducing the system with $S_V = \dfrac{\Lambda_V - \mu_V I_V}{\mu_V} e^{-\tau_{\mu_V}}$ in the final equation, the following system of equations yields the new endemic equilibrium point P_2^*,

$$\begin{aligned}
\frac{dS_H}{dt} &= \Lambda_H - \frac{\beta_1 S_H I_V}{1+\alpha_1 I_V} e^{-\tau_{\mu_V}} - \mu_H S_H, \\
\frac{dI_H}{dt} &= \frac{\beta_1 S_H I_V}{1+\alpha_1 I_V} e^{-\tau_{\mu_V}} - \delta_H I_H - \frac{\gamma u I_H}{1 + buI_H + h} e^{-\tau_{\mu_V}}, \\
\frac{dI_V}{dt} &= \frac{\beta_2 I_H(\Lambda_V - \mu_V I_V)}{\mu_V(1+\alpha_2 I_H)} e^{-\tau_{\mu_V}} - \mu_V I_V.
\end{aligned} \tag{36}$$

As long as the initial conditions are non-negative, we have

$$S_H(0) \geq 0, \quad I_H(0) \geq 0, \quad I_V(0) \geq 0.$$

Theorem 6.1. *The reduced vector-host system (36) with time delay is globally asymptotically stable at the endemic equilibrium point P_2^* whenever $R_0 > 1$.*

Proof. The Jacobian matrix of the system at the endemic equilibrium point P_2^* is given by,

$$J = \begin{bmatrix} -\mu_H - \dfrac{\beta_1 I_V}{1+\alpha_1 I_V} & 0 & -\dfrac{\beta_1 S_V}{(1+\alpha_1 I_V)^2} & -\dfrac{\beta_1 I_V}{1+\alpha_1 I_V} \\ -\mu_H - \delta_H - \dfrac{\gamma u}{(1+buI_H)^2} & 0 & \dfrac{\beta_1 S_V}{(1+\alpha_1 I_V)^2} & \dfrac{\beta_1 I_V}{1+\alpha_1 I_V} \\ 0 & 0 & -\dfrac{\beta_2(\Lambda_V - \mu_V I_V)}{\mu_V(1+\alpha_2 I_H)^2} & \dfrac{\beta_2 I_H}{1+\alpha_2 I_H} \\ 0 & 0 & -\beta_2(1+\alpha_2 I_H) & -\mu_V \end{bmatrix}. \tag{37}$$

We define the subsequent second compound matrix in relation to matrix J as follows,

$$J^{[2]} = \begin{bmatrix} Z_{11} & \beta_1 S_H(1+\alpha_1 I_V)^2 & \beta_1 S_H(1+\alpha_1 I_V)^2 & \beta_2(\Lambda_V - \mu_V I_V)(1+\alpha_2 I_H)^2 \mu_V \\ 0 & Z_{22} & 0 & 0 \\ 0 & 0 & \beta_1 I_V(1+\alpha_1 I_V) & 0 \\ Z_{33} & 0 & 0 & 0 \end{bmatrix}, \tag{38}$$

where

$$\begin{aligned} Z_{11} &= -\gamma u(1+buI_H)^2 - \beta_1 I_V(1+\alpha_1 I_V)e^{-\alpha_1 \tau} - 2\mu_H - \delta_H, \\ Z_{22} &= -\beta_1 I_V(1+\alpha_1 I_V) - \beta_2 I_H(1+\alpha_2 I_H)e^{-\alpha_2 \tau} - \mu_H - \mu_V, \\ Z_{33} &= -\gamma u(1+buI_H)^2 - \beta_2 I_H(1+\alpha_2 I_H)e^{-\alpha_2 \tau} - \delta_H - \mu_H - \mu_V. \end{aligned}$$

The time delays $e^{-\alpha_1 \tau}$ and $e^{-\alpha_2 \tau}$ are incorporated through the exponential terms. To account for the impact of time delay in each element, we introduce a matrix T. The modified expression for T_f and $T_f T^{-1}$ with the introduction of time delay is

$$T_f = \begin{bmatrix} 0 & 0 & 0 \\ 0 & I_V I_H e^{-\alpha_1 \tau} & -I_V e^{-\alpha_2 \tau} \\ 0 & I_H I_V e^{-\alpha_1 \tau} & I_V I_H e^{-\alpha_2 \tau} \end{bmatrix}, \tag{39}$$

and

$$T_f T^{-1} = \begin{bmatrix} 0 & 0 & 0 \\ 0 & I_H e^{-\alpha_1 \tau} & -I_V e^{-\alpha_2 \tau} \\ 0 & I_V e^{-\alpha_1 \tau} & I_H e^{-\alpha_2 \tau} \end{bmatrix}. \tag{40}$$

The matrix $T_f J^{[2]} T^{-1}$ is obtained as,

$$T_f J^{[2]} T^{-1} = \begin{bmatrix} Z_{11} & \beta_1 S_H I_V(1+I_V)^2 I_H & \beta_1 S_H I_V(1+\alpha_1 I_V)^2 I_H \\ Z_{21} & 0 & 0 \\ 0 & \beta_1 I_V(1+\alpha_1 I_V) & Z_{33} \end{bmatrix}, \tag{41}$$

where $Z_{21} = I_H \beta_2(\Lambda_V - \mu_V I_V) I_V(1+\alpha_2 I_H)^2$. The matrix $B = T_f T^{-1} + T_f J^{[2]} T^{-1}$ is split into four blocks,

$$B = \begin{bmatrix} W_{11} & W_{12} \\ W_{21} & W_{22} \end{bmatrix}, \tag{42}$$

where

$$W_{11} = -\mu_H - \delta_H - \gamma u \frac{(1+buI_H)^2}{I_H} - \beta_1 I_H \frac{1+\alpha_1 I_V}{I_H},$$
$$W_{12} = \max\left(\beta_1 S_H I_V \frac{1}{I_H}(1+\alpha_1 I_V)^2, \beta_1 S_H I_V \frac{1}{I_H}(1+\alpha_1 I_V)^2\right),$$
$$W_{21} = I_H \beta_2 (\Lambda_V - \mu_V I_V) \frac{I_V}{\mu_V (1+\alpha_1 I_H)^2},$$
$$W_{22} = \begin{bmatrix} -\beta_2 I_H (1+\alpha_2 I_H) - \mu_H - \beta_1 I_V (1+\alpha_1 I_V) - \mu_V & I_0 I_H - I_{0v} I_V \\ \beta_1 I_V (1+\alpha_1 I_V) - \gamma u (1+buI_H)^2 - \delta_H & I_0 I_V - I_{0h} I_H \end{bmatrix}.$$

Let $\mu(W)$ denote the Lozinski measure, then

$$\mu(W) \leq \sup(f_1, f_2), \tag{43}$$

where the components contributing to f_1 and f_2 are

$$f_1 = \mu(W_{11}) + c,$$
$$f_2 = |W_{21}| + \mu(W_{22}).$$

The Lozinski measure for W_{11} and W_{22} is given by,

$$\mu(W_{11}) = -\mu_H - \delta_H - \gamma u (1+buI_H)^2 - \beta_1 I_V (1+\alpha_1 I_V),$$
$$|W_{21}| = \max\left(\beta_1 S_H I_V \frac{1}{S_H}(1+\alpha_1 I_V)^2, \beta_1 S_H I_V \frac{1}{I_H}(1+\alpha_1 I_V)^2\right).$$

Now,

$$I_{0h} I_H = \frac{I_V I_H \beta_1 S_H}{1+\alpha_1 I_V} - \mu_H - \delta_H - \frac{\gamma u}{1+buI_H}, \tag{44}$$

leading to the expression for f_1,

$$f_1 \leq I_{0h} I_H - \mu_H - \frac{\beta_1 I_V}{1+\alpha_1 I_V}. \tag{45}$$

The expression for $\mu(W_{22})$ with time delay is,

$$\mu(W_{22}) = \sup\left(\begin{array}{l} I_{0h} I_H - I_{0v} I_V - \dfrac{\beta_1 I_V}{1+\alpha_1 I_V} - \dfrac{\beta_2 I_V}{1+\alpha_1 I_V} - \mu_H - \mu_V + \dfrac{\beta_1 I_V}{1+\alpha_1 I_V}, \\ I_{0h} I_H - I_{0v} I_V - K_1 \end{array}\right), \tag{46}$$

where K_1 is a constant. The overall expression for n is given by,

$$n = \lim_{t\to\infty} \sup\left(\frac{1}{t}\int_0^t \mu(W)\, ds\right) \leq \frac{1}{t}\left(I_{0h} I_H - \mu\right). \tag{47}$$

This implies that,

$$n \leq -\mu^2 < 0. \tag{48}$$

Consequently, the examined system is globally asymptotically stable with time delay based on the aforementioned requirements. □

7 The Optimal Control Problem

Using the system (6) with modified birth rates and optimal control variables, the delayed optimal control system becomes,

$$\begin{cases} \dfrac{dS_H}{dt} = \Lambda_H + cN_H - \dfrac{\beta_1 S_H I_V}{1+\alpha_1 I_V}(1-u_1)e^{-\mu_h \tau} - \mu_H S_H, \\ \dfrac{dI_H}{dt} = \dfrac{\beta_1 S_H I_V}{1+\alpha_1 I_V}(1-u_1)e^{-\mu_h \tau} - (\mu_H + \delta_H) I_H - \dfrac{\gamma u_4 I_H}{1+bu_4 I_H} e^{-\mu_h \tau}, \\ \dfrac{dR_H}{dt} = \dfrac{\gamma u_4 I_H}{1+bu_4 I_H} e^{-\mu_h \tau} - \mu_H R_H, \\ \dfrac{dS_V}{dt} = \Lambda_V N_V (1-u_2) e^{-\mu_v \tau} - \dfrac{\beta_2 S_V I_H}{1+\alpha_2 I_H}(1-u_3)e^{-\mu_v \tau} - b_0 u_2 S_V - \mu_V S_V, \\ \dfrac{dI_V}{dt} = \dfrac{\beta_2 S_V I_H}{1+\alpha_2 I_H}(1-u_3)e^{-\mu_v \tau} - \mu_V I_V - b_0 u_2 I_V e^{-\mu_v \tau}. \end{cases} \tag{49}$$

The optimal control variables u_1, u_2, u_3 and u_4 govern the interventions in the system to minimize infection in the human population. The adjusted birth rates and controls allow for a more complete model, considering density impacts and the best methods for disease control. The aim is to reduce infection in the human population. These controls affect the dynamics of the system, and the goal is to determine the optimal distribution for these controls, which leads to,

$$\begin{cases} \dfrac{dS_H}{dt} &= \Lambda_H + cN_H - \dfrac{\beta_1 S_H I_V}{1+\alpha_1 I_V}(1-u_1)e^{-\tau_1 S} - \mu_H S_H, \\ \dfrac{dI_H}{dt} &= \dfrac{\beta_1 S_H I_V}{1+\alpha_1 I_V}(1-u_1)e^{-\tau_2 S} - (\mu_H + \delta_H) I_H - \dfrac{\gamma u_4 I_H}{1+bu_4 I_H} e^{-\tau_2 S}, \\ \dfrac{dR_H}{dt} &= \dfrac{\gamma u_4 I_H}{1+bu_4 I_H} - \mu_H R_H, \\ \dfrac{dS_V}{dt} &= \Lambda_V N_V (1-u_2) e^{-\tau_3 S} - \dfrac{\beta_2 S_V I_H}{1+\alpha_2 I_H}(1-u_3)e^{-\tau_4 S} - b_0 u_2 S_V - \mu_V S_V, \\ \dfrac{dI_V}{dt} &= \dfrac{\beta_2 S_V I_H}{1+\alpha_2 I_H}(1-u_3)e^{-\tau_5 S} - \mu_V I_V - b_0 u_2 I_V e^{-\mu_v \tau}, \\ \dfrac{du_1}{dt} &= 0, \\ \dfrac{du_2}{dt} &= 0, \\ \dfrac{du_3}{dt} &= 0, \\ \dfrac{du_4}{dt} &= 0. \end{cases} \tag{50}$$

Time delays extend the control variables $u(t) = (u_1, u_2, u_3, u_4)$ to $u(t) = (u_1, u_2, u_3, u_4, \tau_1, \tau_2, \tau_3, \tau_4, \tau_5)$ with corresponding Lebesgue measurable constraints,

$$0 \le u_i(t) \le 1, \quad t \in [0, T], \quad i = 1, 2, 3, 4; \quad \tau_i \ge 0, \quad i = 1, 2, 3, 4, 5.$$

The control set is denoted by $\mho = \{(U_1, U_2, U_3, U_4, \tau_1, \tau_2, \tau_3, \tau_4, \tau_5)\}$. Taking into account the time delay factors, the objective function for the vector-host control problem is,

$$J'(u_1, u_2, u_3, u_4, \tau_1, \tau_2, \tau_3, \tau_4, \tau_5) = \int_0^T \left(D_1 I_H + D_2 N_V + \frac{Z'}{2} \right) dt. \tag{51}$$

Here, the constants D_1, D_2, D_3, D_4, D_5, and D_6 represent weight or balancing constants and $Z' = D_3u_1^2 + D_4u_2^2 + D_5u_3^2 + D_6u_4^2$. These constants provide a relative measurement of the interventions over the interval $[0, T]$. The optimal control problem aims to find the control functions $u_i(t)$ and $\tau_i(t)$ that minimize the objective function,

$$J'(u_1^*, u_2^*, u_3^*, u_4^*, \tau_1^*, \tau_2^*, \tau_3^*, \tau_4^*, \tau_5^*) = \max_{\mho} J(u_1, u_2, u_3, u_4, \tau_1, \tau_2, \tau_3, \tau_4, \tau_5). \tag{52}$$

8 Existence of the Optimality System

To demonstrate the existence of the control problem, the optimal control system (49) is outlined as follows,

Case 1: Verify that the system (49) is not empty for both the state and control variables.

Case 2: Confirm that the control set U is open and concave.

Case 3: Ensure that the equation on the right-hand side of system (49) is bounded, continuous, and expressible as a linear function of u, with coefficients that depend on time and size.

Case 4: The integrand $L(y', u', t')$ of the objective function J' is concave and satisfies the following inequality because there are constants $l_1, l_2 > 0$ and $m^* > 1$,

$$l_1 = \left(\|u_1\|^2 + \|u_2\|^2 + \|u_3\|^2\right)^{\frac{m^*}{2}} - l_2.$$

To validate **Case 1**, the state variables and controls are constrained in these circumstances (**Case 1** – **Case 4**). The model is bilinear in the control variables to satisfy **Case 3**. For **Case 4** and its verification, the final condition is,

$$D_1I_H + D_2N_V + \frac{1}{2}\sum_{i=3}^{6} D_iu_i^2 \geq l_1\left(|u_1|^2 + |u_2|^2 + |u_3|^2 + |u_4|^2\right)^{\frac{m^*}{2}} - l_2,$$

where for $i = 1, \ldots, 6$, $D_i, l_1, l_2 > 0, m^* > 1$.

Theorem 8.1. *Let $X_d = \big(S_H, I_H, R_H, S_V, I_V, S_H(\tau), I_H(\tau), R_H(\tau), S_V(\tau), I_V(\tau)\big)$ represent the state vector with a time delay τ for each compartment. Similarly, extend the control vector to include delayed controls,*

$$\mho_d = \big(u_1, u_2, u_3, u_4, u_1(\tau), u_2(\tau), u_3(\tau), u_4(\tau)\big).$$

Define the Lagrangian L_d and the Hamiltonian H_d for the optimal control problem, taking time delays into account,

$$\begin{aligned} L_d &= D_1I_H + D_2N_V \\ &\quad + \frac{1}{2}\Big[D_3u_1^2 + D_4u_2^2 + D_5u_3^2 + D_6u_4^2 + D_7u_1(\tau)^2 + D_8u_2(\tau)^2 + D_9u_3(\tau)^2 + D_{10}u_4(\tau)^2\Big]. \end{aligned} \tag{53}$$

The corresponding Hamiltonian is,

$$H_d(X_d, \mho_d, \Lambda) = L_d + \sum_{i=1}^{5} \Lambda_j\left(\frac{dX_i}{dt} - X_j\right) + \sum_{i=1}^{5} \Lambda_{i+5}\left(\frac{dX_i}{dt} - X_i(t)\right), \tag{54}$$

where $\Lambda = (\Lambda_1, \Lambda_2, \ldots, \Lambda_{10})$ is the vector of Lagrange multipliers. This formulation ensures that the dynamics of the system, including time delays, are fully represented in the optimal control solution.

9 Solution to the Optimal Control Problem

Using Pontryagin's Maximum Principle [23] for the solution of optimality system (49). Let u_i^*, for $i = 1, 2, 3, 4$ denote the optimal solution, then the adjoint variables say λ_i, for $i = 1, 2, \ldots, 10$ exists. Let, $\Lambda_d = (\lambda_1, \lambda_2, \lambda_3, \lambda_4, \lambda_5, \lambda_6, \lambda_7, \lambda_8, \lambda_9, \lambda_{10})$ represent the adjoint vector with time delays. Similarly, let,

$$\frac{d\Lambda}{dt}(\tau) = \left(\frac{d\lambda_1}{d\tau}, \frac{d\lambda_2}{d\tau}, \ldots, \frac{d\lambda_{10}}{d\tau}\right),$$

denote the delayed adjoint variables. Now, the adjoint system with time delays becomes,

$$\begin{aligned} \frac{dx}{dt} &= \frac{\partial H_d}{\partial \Lambda_d}, \\ 0 &= \frac{\partial H_d}{\partial \mho_d}, \\ \frac{d\Lambda_d}{dt} &= -\frac{\partial H_d}{\partial X_d}. \end{aligned} \tag{55}$$

These equations capture the dynamics of the adjoint variables, accounting for the time delays in both state and adjoint variables. Using these conditions in H_d, we obtain a set of equations that form the basis for solving the optimal control problem with time delays.

Theorem 9.1. *In order to obtain results for the adjoint system (54) and the transversality condition, we solve the control system in conjunction with the Hamiltonian H(54) for $S_H = S_H^*$, $I_H = I_H^*$, $R_H = R_H^*$, $S_V = S_V^*$, $I_V = I_V^*$. The expression in (54) is the derivative of H with respect to S_H, I_H, R_H, S_V, I_V. The criterion $\dfrac{\partial H}{\partial u_i} = 0$ is applied to the optimal control characterization equations for $i = 1, \ldots, 4$. Using the adjoint variables and other parameters, this leads to the precise formula for the adjoint-controlled variables u_i^*.*

Proof. The system equation with time delay (49) in the Hamiltonian can be expressed as,

$$\begin{aligned} \dot{S_H} &= \Lambda_H + cN_H - \frac{\beta_1 S_H I_V(t-\tau)}{1+\alpha_1 I_V(t-\tau)}(1-u_1(t-\tau)) - \mu_H S_H, \\ \dot{I_H} &= \frac{\beta_1 S_H I_V(t-\tau)}{1+\alpha_1 I_V(t-\tau)}(1-u_1(t-\tau)) - (\mu_H+\delta_H) I_H - \frac{\gamma u_4 I_H}{1+bu_4 I_H}, \\ \dot{R_H} &= \frac{\gamma u_4 I_H}{1+bu_4 I_H} - \mu_H R_H, \\ \dot{S_V} &= \Lambda_V N_V(t-\tau)(1-u_2(t-\tau)) - \frac{\beta_2 S_V I_H(t-\tau)}{1+\alpha_2 I_H(t-\tau)}(1-u_3(t-\tau)) - \mu_V S_V - b_0 u_2 S_V, \\ \dot{I_V} &= -\frac{\beta_2 S_V I_H(t-\tau)}{1+\alpha_2 I_H(t-\tau)}(1-u_3(t-\tau)) - \mu_V I_V - b_0 u_2 I_V. \end{aligned} \tag{56}$$

The optimal control system equations with time delay are

$$\begin{aligned}
\dot{\lambda_1} &= -\frac{\partial H}{\partial S_H} = 0,\\
\dot{\lambda_2} &= -\frac{\partial H}{\partial I_H} = 0,\\
\dot{\lambda_3} &= -\frac{\partial H}{\partial R_H} = 0,\\
\dot{\lambda_4} &= -\frac{\partial H}{\partial S_V} = 0,\\
\dot{\lambda_5} &= -\frac{\partial H}{\partial I_V} = 0.
\end{aligned} \tag{57}$$

The Hamiltonian H is given by,

$$\begin{aligned}
H = {} & D_1 H_H + D_2 N_V + \frac{1}{2} D_3 u_1^2 + \frac{1}{2} D_4 u_2^2 + \frac{1}{2} D_5 u_3^2 + \frac{1}{2} D_6 u_4^2 + \lambda_1 \dot{S_H} + \lambda_2 \dot{I_H} + \lambda_3 \dot{R_H}\\
& + \lambda_4 \dot{S_V} + \lambda_5 \dot{I_V}.
\end{aligned} \tag{58}$$

The ideal controls are provided by,

$$\begin{aligned}
u_1^* &= \min\left\{0, \max\left\{1, (\lambda_2 - \lambda_1)\frac{\beta_1 S_H I_V}{(1+\alpha_1 I_V) D_3}\right\}\right\},\\
u_2^* &= \min\left\{0, \max\left\{1, \lambda_4 \Lambda_V N_V + b_0 S_V + \lambda_5 b_0 I_V D_4\right\}\right\},\\
u_3^* &= \max\left\{0, \min\left\{1, (\lambda_5 - \lambda_4)\frac{\beta_2 S_V I_H}{(1+\alpha_2 I_H) D_5}\right\}\right\},\\
u_4^* &= \max\left\{0, \min\left\{1, (\lambda_3 - \lambda_2)\frac{\gamma I_H}{(1+b u_4 I_H)^2 D_6}\right\}\right\}.
\end{aligned} \tag{59}$$

The requirements for transversality are

$$\dot{\lambda_1}(T_f'(\tau)) = \dot{\lambda_2}(T_f'(\tau)) = \dot{\lambda_3}(T_f'(\tau)) = \dot{\lambda_4}(T_f'(\tau)) = \dot{\lambda_5}(T_f'(\tau)) = 0. \tag{60}$$

Thus, the optimal control system results in a modified set of equations for the adjoint variables and optimal controls. While the provided equations involve intricate mathematical expressions, a specific formulation of the time delay is necessary for detailed analysis. Consequently, the structure of the equations will depend on the specific form of the time delay, ensuring that optimal control integration in the influenced model is stable. □

10 Numerical Simulation

This section presents a detailed stability analysis of the human populations (susceptible, infected, and recovered) within a vector-host disease model, incorporates time delays and a saturated treatment capacity. The objective is to determine the conditions under which the disease dynamics exhibit stability around the endemic and disease-free equilibria, both locally and globally. Numerical simulations are used to validate these theoretical results.

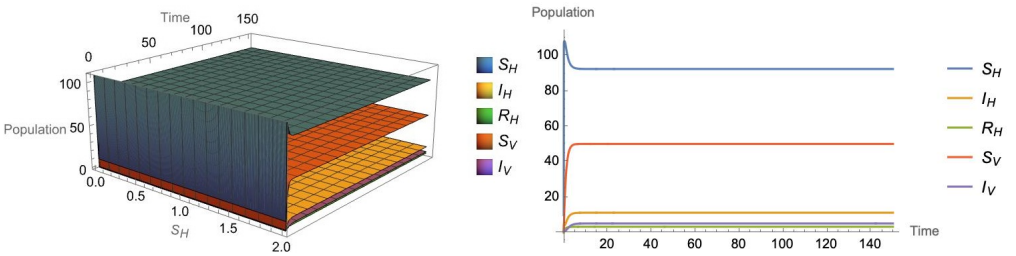

Figure 1: Stability analysis of S_H in a delayed vector-host disease model: (a) 3D plot view and (b) 2D plot view.

Figure 1 illustrates plausible situations in which overcrowding in the healthcare system might result in treatment capacity limitation. To mimic the effects of increased treatment efforts and preventative measures, the control function adjusts the recovery rate and potentially the transmission rates. When successful control methods are implemented, the models show a significant decline in the number of afflicted humans. When treatment capacity is sufficiently enhanced to manage the infected population without reaching saturation, this decline becomes more noticeable. Initially, the susceptible population may decrease due to infection, but as more individuals recover or receive appropriate treatment, the population either stabilizes or grows. Efficient treatment reduces the number of sick individuals and increases recovery rates, there is a noticeable rise in the recovered population, denoted by parameters such as $\Lambda_1 = 9894$, $\Lambda_2 = 50$, $\mu_1 = 83$, $\mu_2 = 0.9$, $\gamma = 90$, $\delta_1 = 0.4$, $\beta_1 = 90$, $\beta_2 = 0.027$, $b = 0.232667$, $u = 1$, $\alpha_1 = 0.3$, $\alpha_2 = 0.2$. Reducing the vector population is essential for breaking the transmission cycle. As the number of infected individuals rapidly decreases and the number of recovered individuals increases, the overall prevalence of the illness declines. These results support the theoretical predictions of stability analysis and emphasize the importance of timely and effective control measures in managing vector-host infections [10, 30].

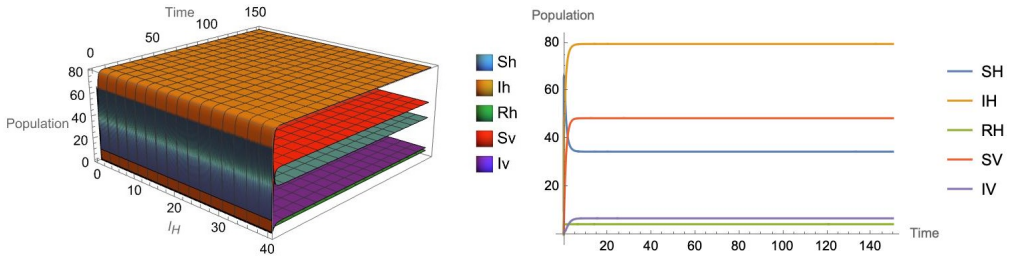

Figure 2: Stability analysis of I_H in a delayed vector-host disease model: (a) 3D plot view and (b) 2D plot view.

Figure 2 shows that the improved treatment capacity initially leads to a decrease in the number of afflicted humans. But over time, the decline is not sustained since the management technique has little impact on the vector populations that spread the illness. While there is a modest increase in the vulnerable human population, but no significant difference is observed. This implies that the control technique is not effective in preventing the spread of new illnesses. Although the number of people who have recovered increases, indicating improved treatment efforts, the constant influx of new infections through the vectors cancels this progress. The simulations show that there is little change in the vector populations. A never-ending cycle of new infections is caused by the lack of impact on the vector populations and the vulnerable human population, despite the initial decrease in the number of sick humans [32].

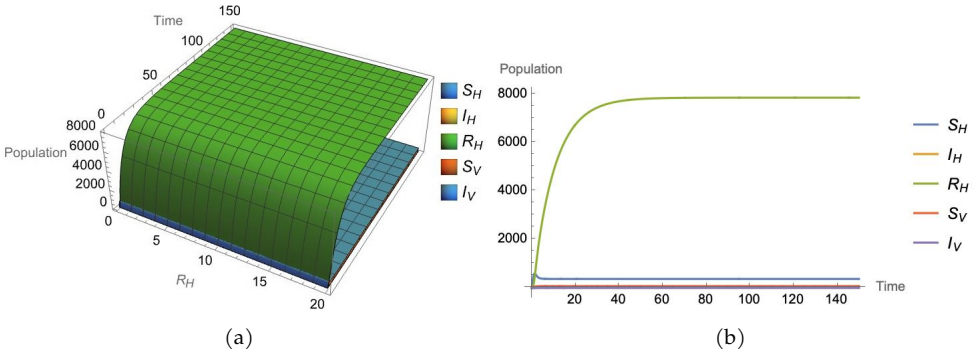

Figure 3: Stability analysis of R_H in a delayed vector-host disease model: (a) 3D plot view and (b) 2D plot view.

Figure 3 illustrates how the present management technique results in an increase in the vulnerable vector population. This suggests that the existing controls are not successfully lowering the population of vectors, which is increasing the quantity of vectors that can spread the illness. The fact that more people are being sick further indicates that the control technique is not effectively breaking the cycle of vector-human transmission. This might be because vector control measures are not implemented enough or their effects take longer to manifest. The high recruiting rate compared to the rate of new infections probably causes the dramatic growth in the vulnerable human population. This suggests that the infection pressure from the vector population is high even when there is an increase in the number of individuals by the ratio $\Lambda_1 = 10$, $\Lambda_2 = 50$, $\mu_1 = 83$, $\mu_2 = 0.1$, $\gamma = 0.3$, $\delta_1 = 0.4$, $\beta_1 = 0.25$, $\beta_2 = 0.025$, $b = 1/60$, $u = 1$, $\alpha_1 = 0.3$, $\alpha_2 = 0.2$ in the vulnerable pool. A measure of the success of treatment and recovery efforts may be seen in the rise in the number of recovered humans. The number of infected vectors is growing, suggesting that there is still a significant level of human-to-vector transmission. This may result from inadequately lowering the transmission rates or vector populations by actions that are not being implemented promptly or from inefficient vector control tactics [33].

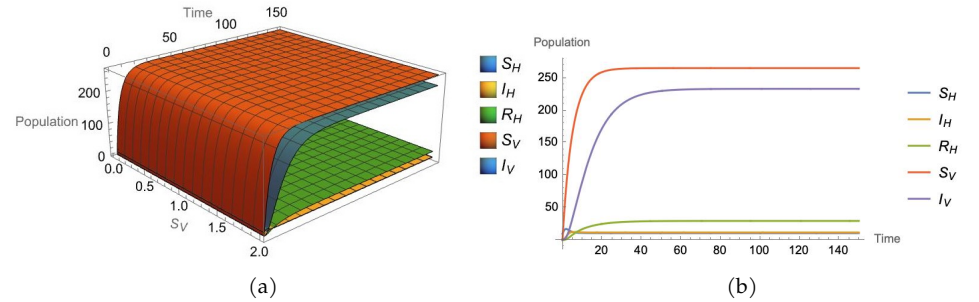

Figure 4: Stability analysis of S_V in a delayed vector-host disease model: (a) 3D plot view and (b) 2D plot view.

Figure 4 shows how the susceptible human population is increasing as a result of the management strategy's ability to reduce the number of infected vectors. This rise indicates that fewer new infections are reaching the susceptible population. Regarding the infected human population, it appears that the decrease in the number of infected vectors significantly reduces the rate of transmission to humans. This outcome demonstrates the effectiveness of the control techniques in breaking the transmission cycle. The control method has no direct effect on the recovery rate, as the number of recovered individuals remains unchanged even as the infection rate decreases. This constancy suggests that treatment efforts are ongoing, with the primary effect being a reduced infection rate. As the number of infected vectors decreases, the susceptible vector population may

increase or remain stable due to reduced competition and increased availability of resources. This result is a direct consequence of effective vector control measures. As evidenced by the significant drop in the infected vector population, vector management measures have reduced the number of vectors capable of spreading the illness. This reduction is crucial in minimizing the impact of infections on the human population. The increase in the susceptible human population, resulting from the disruption of the vector-to-human transmission cycle, suggests a decline in the rate of new infections. A reduced population of infected vectors means fewer infected humans, which in turn leads to lower transmission rates. Ongoing treatment efforts are reflected in the steady number of recovered cases, while the management strategy primarily reduces, rather than increases, the rate of new infections. The vector component of the disease cycle has been successfully reduced by vector control approaches, as seen by the significant drop in the infected vector population.

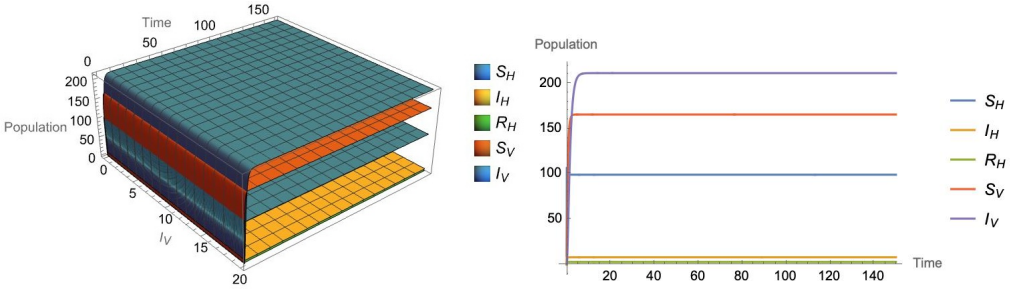

Figure 5: Stability analysis of I_V in a delayed vector-host disease model: (a) 3D plot view and (b) 2D plot view.

Figure 5 illustrates how the management method lowers the incidence of new infections, leading to an increase in the vulnerable human population. This rise, indicative of effective preventive efforts, shows that fewer people are moving from the susceptible to the infected group. The infected human population declines, indicating that the control methods are successful in reducing the transmission rate and increasing the recovery rate. The greater number of recovered individuals further demonstrates the effectiveness of the control technique in improving recovery. This improvement is the result of better healthcare interventions and treatments, which have increased the number of people recovering from infection. As the number of infected vectors declines, the susceptible vector population may increase. This suggests that although the vectors are still present, their ability to spread the illness is diminished, as reflected in parameters such as $\Lambda_1 = 10$, $\Lambda_2 = 50$, $\mu_1 = 0.1$, $\mu_2 = 0.1$, $\gamma = 90$, $\delta_1 = 0.4$, $\beta_1 = 0.25$, $\beta_2 = 0.025$, $b = 1/60$, $u = 1$, $\alpha_1 = 0.3$, $\alpha_2 = 0.2$, which results in fewer new infections in humans. The sharp reduction in the infected vector population demonstrates the efficacy of vector control techniques in limiting the spread of the disease to humans. The significant rise in the recovered population indicates the success of enhanced treatment programs and medical interventions. The decrease in the infected human population shows that the management methods are effective in halting transmission and promoting recovery. As a result of effective preventive measures, there are fewer new infections, as evidenced by the increase in the susceptible population. The reduction in the number of infected vectors underscores the importance of vector management strategies in breaking the cycle of transmission.

In Figure 6, the comparison of vector-host coexistence shows an unmanaged situation with a significant rise in the vulnerable human population. This increase indicates that efforts to prevent infections have been successful in lowering the rate of new infections. Under the control methods, the number of infected humans declines dramatically, demonstrating that improved treatment capacity and reduced transmission rates are effectively decreasing the infected population. In the controlled situation, the population of recovered humans rises significantly, reflecting a larger

number of individuals moving from infection to recovery due to enhanced treatment capacity and improved recovery rates.

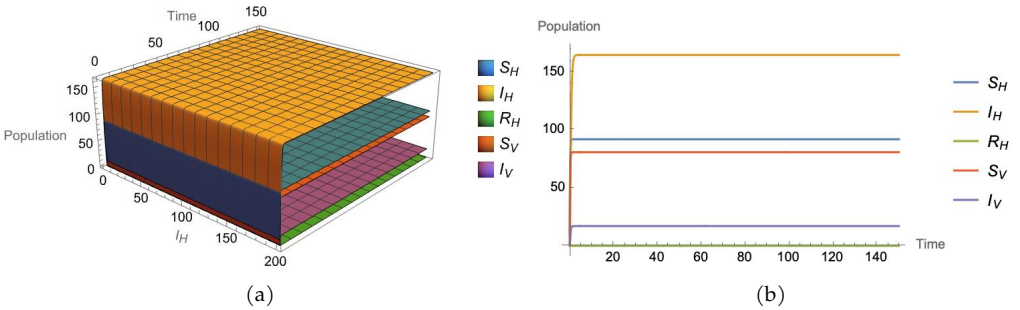

Figure 6: Coexistence of stability analysis in delayed vector-host disease-1: (a) 3D plot view and (b) 2D plot view.

Under the management procedures, with parameters $\Lambda_1 = 422$, $\Lambda_2 = 500$, $\mu_1 = 0.1$, $\mu_2 = 5.1$, $\gamma = 0.4$, $\delta_1 = 2.4$, $\beta_1 = 4.2935$, $\beta_2 = 0.7595$, $b = 1000$, $u = 0.1$, $\alpha_1 = 0.9$, $\alpha_2 = 0.7$, the number of vulnerable vectors declines. This decrease highlights the effectiveness of vector control tactics in reducing the number of vectors at risk of becoming infected. In the controlled setting, the population of infected vectors drops drastically. Effective vector control strategies lower the infection burden by reducing the number of vectors capable of transmitting the disease to humans. The overall control technique greatly improves the coexistence and stability of the various population compartments in the disease model.

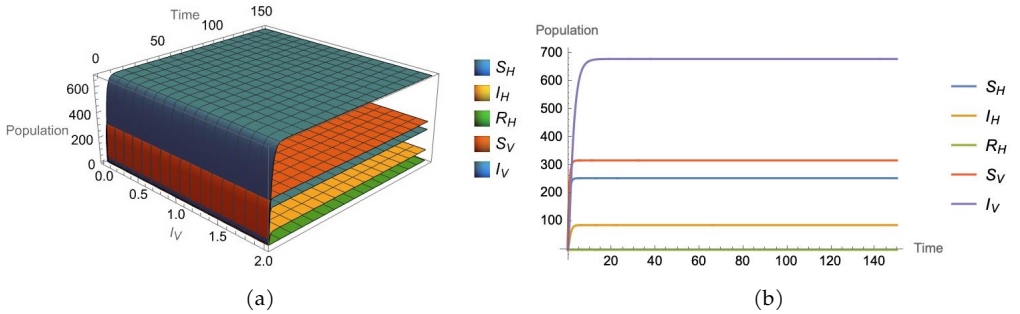

Figure 7: Coexistence of stability analysis in delayed vector-host disease-2: (a) 3D plot view and (b) 2D plot view.

Figure 7 shows a significant rise in the number of susceptible and recovered humans, suggesting that the control methods are effectively improving recovery rates and successfully preventing new infections. The notable reduction in the number of afflicted individuals indicates the efficacy of the control methods in mitigating transmission and promoting recovery. The decline in both the susceptible and infected vector populations further emphasizes the success of the vector control strategies, with parameters $\Lambda_1 = 422$, $\Lambda_2 = 500$, $\mu_1 = 1.1$, $\mu_2 = 0.5$, $\gamma = 1.4$, $\delta_1 = 0.5$, $\beta_1 = 4.975$, $\beta_2 = 0.7595$, $b = 900$, $u = 0.5$, $\alpha_1 = 0.9$, $\alpha_2 = 0.7$, in disrupting the transmission cycle and reducing the risk of infection. By contrasting the controlled situation with the uncontrolled baseline, it is evident that the integrated control technique produces a more stable and favorable outcome for managing the vector-host disease dynamics.

Figure 8 shows oscillatory behavior, varying around a point of equilibrium, according to the simulations. The temporal lags in the transmission mechanism and the nonlinear feedback between the susceptible and infected populations are responsible for these oscillations. As the vul-

nerable population grows, more people become sick. The infected human population shows only slight variations in response to these oscillations, remaining largely steady. Although the vulnerable population fluctuates, the stability indicates that the overall infection rate is under control. Oscillatory behavior is also observed in the recovered human population, with fluctuations occurring as more individuals recover after contracting the virus. The recovery rate stabilizes as the number of new infections decreases.

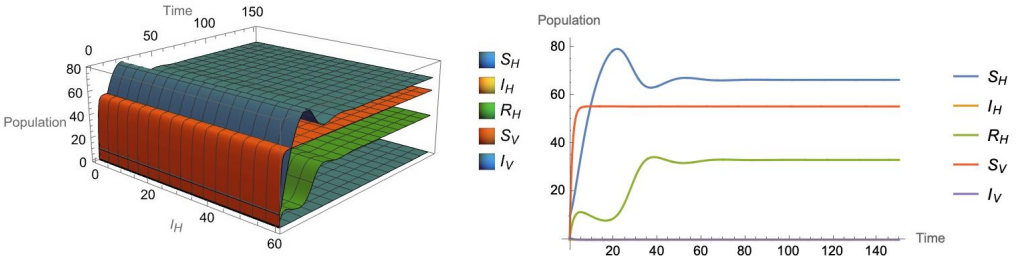

(a) (b)

Figure 8: Oscillations of disease transmission in population dynamics: (a) 3D plot view and (b) 2D plot view.

The susceptible vector population does not exhibit fluctuations, suggesting that the vector control strategies are effective and prevent oscillatory behavior in the vector population. Similarly, the population of infected vectors remains relatively unchanged. According to the stability, with parameters $\Lambda_1 = 10$, $\Lambda_2 = 50$, $\mu_1 = 0.1$, $\mu_2 = 0.9$, $\gamma = 90$, $\delta_1 = 0.4$, $\beta_1 = 0.903$, $\beta_2 = 0.025$, $b = 0.0166667$, $u = 1$, $\alpha_1 = 0.3$, $\alpha_2 = 0.2$, the infected vector population can be effectively managed through vector control techniques. The oscillations reflect the dynamics of the infection interacting with the delayed recovery process. Despite the fluctuations in susceptible and recovered populations, the relative stability implies that overall infection rates remain under control, which is crucial for preventing large-scale epidemics.

The interaction between time delays and nonlinear dynamics in the vector-host disease model can lead to oscillatory behavior in both the susceptible and recovered human populations, as shown in the numerical simulations. Understanding the factors contributing to this oscillatory behavior can help in better planning public health interventions, ensuring the management of vector-host diseases in a stable and advantageous manner.

11 Advantages and Limitations

Time delays and treatment saturation add realism to disease models by simulating real-world delays in symptom development or treatment progression, as well as the constraints on medical resources during pandemics. These factors enhance the understanding of disease dynamics and help in predicting how diseases will spread when faced with challenges such as limited resources or delayed treatments. By modeling various scenarios, the model aids policymakers in developing more effective control strategies. Stability analysis further optimizes interventions by providing insights into how equilibrium states, such as the basic reproduction number (R_0), change with parameter adjustments.

However, time delays and saturation increase system complexity, making it harder to derive

analytical solutions, often requiring the use of numerical methods that may offer less intuitive understanding. The inclusion of additional factors, such as treatment limitations and delay duration, complicates accurate estimation, especially when data is scarce. While these complexities can make the model more realistic, they can also obscure the underlying dynamics. Additionally, incorporating too many processes can lead to overfitting, which limits the model's generalizability to other populations or conditions.

Future research can integrate stochastic dynamics [6] into our vector-host disease model by incorporating environmental and demographic noise through Wiener and Poisson processes to increase the model's robustness and applicability. Stability analysis would employ stochastic methods, and optimal control could be refined using the Hamilton-Jacobi-Bellman equation. Numerical simulations, such as the Euler-Maruyama scheme, would assess the impact of stochastic fluctuations on treatment strategies, enhancing model accuracy in predicting outcomes and devising optimal interventions. Key challenges, including parameter estimation, computational complexity, and uncertainty quantification, will provide valuable insights into managing vector-host diseases in practical applications.

12 Conclusion

The mathematical model of vector-host illness is examined, with an expansion to include the temporal dynamics of disease transmission and prevention measures. The stability analysis provides a deeper understanding of the system's behavior in both endemic and disease-free scenarios, particularly when time delay is considered. Additionally, the optimum control problem with time delay and saturated treatment functions is designed and formulated using control variables. The influence of delayed therapies on disease dynamics is revealed by simulation findings that incorporate time delay into the optimum control framework. These findings clarify the complex interactions between temporal factors and the most effective strategies for controlling vector-host illnesses, thereby enhancing the model's accuracy.

Acknowledgement The authors express their sincere gratitude to the referees for their insightful comments and constructive suggestions, which have significantly contributed to the improvement of this work.

Conflicts of Interest The authors declare no conflicts of interest. This work did not receive any funding.

References

[1] M. A. Acevedo, O. Prosper, K. Lopiano, N. Ruktanonchai, T. T. Caughlin, M. Martcheva, C. W. Osenberg & D. L. Smith (2015). Spatial heterogeneity, host movement and mosquito-borne disease transmission. *PloS One*, *10*(6), Article ID: e0127552. https://doi.org/10.1371/journal.pone.0127552.

[2] B. Adams & D. D. Kapan (2009). Man bites mosquito: Understanding the contribution of human movement to vector-borne disease dynamics. *PloS One*, *4*(8), Article ID: e6763. https://doi.org/10.1371/journal.pone.0006763.

[3] F. B. Agusto & M. A. Khan (2018). Optimal control strategies for dengue transmission in Pakistan. *Mathematical Biosciences*, *305*, 102–121. https://doi.org/10.1016/j.mbs.2018.09.007.

[4] S. A. Alavi Saeed & A. Heydari (2015). Numerical solution of a class of nonlinear optimal control problems. *Malaysian Journal of Mathematical Sciences*, *9*(2), 259–275.

[5] D. Aldila, T. Götz & E. Soewono (2013). An optimal control problem arising from a dengue disease transmission model. *Mathematical Biosciences*, *242*(1), 9–16. https://doi.org/10.1016/j.mbs.2012.11.014.

[6] S. Bera, S. Khajanchi & T. K. Kar (2024). Stochastic persistence, extinction and stationary distribution in HTLV-I infection model with CTL immune response. *Qualitative Theory of Dynamical Systems*, *23*(Suppl 1), Article ID: 265. https://doi.org/10.1007/s12346-024-01120-x.

[7] S. Bera, S. Khajanchi & T. K. Roy (2022). Dynamics of an HTLV-I infection model with delayed CTLs immune response. *Applied Mathematics and Computation*, *430*, Article ID: 127206. https://doi.org/10.1016/j.amc.2022.127206.

[8] S. Bera, S. Khajanchi & T. K. Roy (2023). Stability analysis of fuzzy HTLV-I infection model: A dynamic approach. *Journal of Applied Mathematics and Computing*, *69*(1), 171–199. https://doi.org/10.1007/s12190-022-01741-y.

[9] M. H. A. Biswas, L. T. Paiva & M. de Pinho (2014). A SEIR model for control of infectious diseases with constraints. *Mathematical Biosciences & Engineering*, *11*(4), 761–784. https://doi.org/10.3934/mbe.2014.11.761.

[10] L. M. Cai, X. Z. Li, B. Fang & S. Ruan (2017). Global properties of vector-host disease models with time delays. *Journal of Mathematical Biology*, *74*, 1397–1423. https://doi.org/10.1007/s00285-016-1047-8.

[11] D. K. Das, S. Khajanchi & T. K. Kar (2020). Transmission dynamics of tuberculosis with multiple re-infections. *Chaos, Solitons & Fractals*, *130*, Article ID: 109450. https://doi.org/10.1016/j.chaos.2019.109450.

[12] A. Dwivedi, R. Keval & S. Khajanchi (2022). Modeling optimal vaccination strategy for dengue epidemic model: A case study of India. *Physica Scripta*, *97*(8), Article ID: 085214. https://doi.org/10.1088/1402-4896/ac807b.

[13] M. Eder, F. Cortes, N. Teixeira de Siqueira Filha, G. V. Araújo de França, S. Degroote, C. Braga, V. Ridde & C. M. Turchi Martelli (2018). Scoping review on vector-borne diseases in urban areas: Transmission dynamics, vectorial capacity and co-infection. *Infectious Diseases of Poverty*, *7*(1), Article ID: 90. https://doi.org/10.1186/s40249-018-0475-7.

[14] S. M. Garba, A. B. Gumel & M. R. A. Bakar (2008). Backward bifurcations in dengue transmission dynamics. *Mathematical Biosciences*, *215*(1), 11–25. https://doi.org/10.1016/j.mbs.2008.05.002.

[15] A. Jabbari, M. Lotfi, H. Kheiri & S. Khajanchi (2023). Mathematical analysis of the dynamics of a fractional-order tuberculosis epidemic in a patchy environment under the influence of re-infection. *Mathematical Methods in the Applied Sciences*, *46*(17), 17798–17817. https://doi.org/10.1002/mma.9532.

[16] S. Khajanchi, S. Bera & T. K. Roy (2021). Mathematical analysis of the global dynamics of a HTLV-I infection model, considering the role of cytotoxic T-lymphocytes. *Mathematics and Computers in Simulation*, *180*, 354–378. https://doi.org/10.1016/j.matcom.2020.09.009.

[17] S. Khajanchi, D. K. Das & T. K. Kar (2018). Dynamics of tuberculosis transmission with exogenous reinfections and endogenous reactivation. *Physica A: Statistical Mechanics and Its Applications*, *497*, 52–71. https://doi.org/10.1016/j.physa.2018.01.014.

[18] S. Khajanchi, K. Sarkar & S. Banerjee (2022). Modeling the dynamics of COVID-19 pandemic with implementation of intervention strategies. *The European Physical Journal Plus*, *137*(1), Article ID: 129. https://doi.org/10.1140/epjp/s13360-022-02347-w.

[19] M. A. Khan, N. Iqbal, Y. Khan & E. Alzahrani (2020). A biological mathematical model of vector-host disease with saturated treatment function and optimal control strategies. *Mathematical Biosciences and Engineering*, *17*(4), 3972–3997. https://doi.org/10.3934/mbe.2020220.

[20] R. Kumar Rai, P. Kumar Tiwari & S. Khajanchi (2023). Modeling the influence of vaccination coverage on the dynamics of COVID-19 pandemic with the effect of environmental contamination. *Mathematical Methods in the Applied Sciences*, *46*(12), 12425–12453. https://doi.org/10.1002/mma.9185.

[21] T. Y. Miyaoka, S. Lenhart & J. F. Meyer (2019). Optimal control of vaccination in a vector-borne reaction–diffusion model applied to Zika virus. *Journal of Mathematical Biology*, *79*(3), 1077–1104. https://doi.org/10.1007/s00285-019-01390-z.

[22] J. Mondal & S. Khajanchi (2022). Mathematical modeling and optimal intervention strategies of the COVID-19 outbreak. *Nonlinear Dynamics*, *109*(1), 177–202. https://doi.org/10.1007/s11071-022-07235-7.

[23] J. Mondal, S. Khajanchi & P. Samui (2022). Impact of media awareness in mitigating the spread of an infectious disease with application to optimal control. *The European Physical Journal Plus*, *137*(8), Article ID: 983. https://doi.org/10.1140/epjp/s13360-022-03156-x.

[24] R. M. Neilan & S. Lenhart (2010). *Modeling Paradigms and Analysis of Disease Trasmission Models*, volume 75, chapter An Introduction to Optimal Control with an Application in Disease Modeling, pp. 67–81. American Mathematical Society, South Africa. https://doi.org/10.1090/dimacs/075.

[25] I. Ratti & P. Kalra (2023). Study of disease dynamics of co-infection of Rotavirus and Malaria with control strategies. *Malaysian Journal of Mathematical Sciences*, *17*(2), 151–177. https://doi.org/10.47836/mjms.17.2.05.

[26] S. F. Sadiq, M. A. Khan, S. Islam, G. Zaman, I. H. Jung & S. A. Khan (2014). Optimal control of an epidemic model of leptospirosis with nonlinear saturated incidences. *Annual Research & Review in Biology*, *4*(3), 560–576. https://doi.org/10.9734/ARRB/2014/6378.

[27] K. Sarkar, J. Mondal & S. Khajanchi (2022). How do the contaminated environment influence the transmission dynamics of COVID-19 pandemic? *The European Physical Journal Special Topics*, *231*(18), 3697–3716. https://doi.org/10.1140/epjs/s11734-022-00648-w.

[28] D. L. Smith, K. E. Battle, S. I. Hay, C. M. Barker, T. W. Scott & F. E. McKenzie (2012). Ross, Macdonald, and a theory for the dynamics and control of mosquito-transmitted pathogens. *PLoS Pathogens*, *8*(4), Article ID: e1002588. https://doi.org/10.1371/journal.ppat.1002588.

[29] P. Thongsripong, J. M. Hyman, D. D. Kapan & S. N. Bennett (2021). Human–mosquito contact: A missing link in our understanding of mosquito-borne disease transmission dynamics. *Annals of the Entomological Society of America*, *114*(4), 397–414. https://doi.org/10.1093/aesa/saab011.

[30] S. Ullah, M. F. Khan, S. A. A. Shah, M. Farooq, M. A. Khan & M. b. Mamat (2020). Optimal control analysis of vector-host model with saturated treatment. *The European Physical Journal Plus*, *135*(10), Article ID: 839. https://doi.org/10.1140/epjp/s13360-020-00855-1.

[31] X. Wang, Y. Chen & S. Liu (2018). Global dynamics of a vector-borne disease model with infection ages and general incidence rates. *Computational and Applied Mathematics*, *37*, 4055–4080. https://doi.org/10.1007/s40314-017-0560-8.

[32] H. M. Wei, X. Z. Li & M. Martcheva (2008). An epidemic model of a vector-borne disease with direct transmission and time delay. *Journal of Mathematical Analysis and Applications*, *342*(2), 895–908. https://doi.org/10.1016/j.jmaa.2007.12.058.

[33] R. Zhang, D. Li & Z. Jin (2015). Dynamic analysis of a delayed model for vector-borne diseases on bipartite networks. *Applied Mathematics and Computation*, *263*, 342–352. https://doi.org/10.1016/j.amc.2015.04.074.